04

Application of the fusion reaction diagnostics for observing rearrangement of the fast-particle distribution function at the Gas Dynamic Trap

© E.I. Pinzhenin

Budker Institute of Nuclear Physics, Siberian Branch, Russian Academy of Sciences, Novosibirsk, Russia
E-mail: e.i.pinzhenin@inp.nsk.su

Received June 23, 2025
Revised September 2, 2025
Accepted September 3, 2025

The paper presents the first GDT experiments on evolution of the spatial profile of fusion proton emission as a result of the Alfven ion-cyclotron instability. Such a redistribution is a consequence of variations in the fast-ion distribution function. As the recorders, a system of fusion proton detectors was used; the distribution function was modeled by using the DOL code.

Keywords: Gas Dynamic Trap, fast ions, fusion reaction diagnostics.

DOI: 10.61011/TPL.2026.01.62820.20413

The Gas Dynamic Trap (GDT) is an open axisymmetric magnetic system designed for confining plasma with subthermonuclear parameters (Fig. 1, *a*) [1,2]. GDT was created and is now employed at the Institute of Nuclear Physics SB RAS (Novosibirsk). The GDT research program is aimed at justifying thermonuclear applications of the next-generation open axisymmetric trap, namely, a neutron source and fusion reactor based on it. The GDT experiment distinctive feature is formation of plasma consisting of two components with strongly different parameters. The target plasma (hydrogen or deuterium) with the temperature and concentration of $3-10$ eV and $(1-7)\cdot 10^{14}$ cm^{-3}, respectively, is created by using an arc source installed in one of the GDT expanders [3]. Further, as a result of operation of a set of atomic injectors, electrons become heated to 250 eV (up to 1 keV in experiments with microwave heating) [4], and this plasma component is confined in the collisional mode. The fast ion population is formed as a result of high-power injection of deuterium atoms into the trap. The heating system operating time is 5 ms. Average energy of fast plasma ions is 10 keV, maximum energy matches the injection energy of 22 keV, while the concentration is up to $2\cdot 10^{13}$ cm^{-3}. Calculations of the fast ion concentration are presented in Fig. 1, *c*. In this study, the concentration was calculated using program code DOL [5]; as input data, the setup geometric dimensions and characteristics, magnetic field profile, atomic injection parameters, and other quantities were used. Fast ions are confined in the collision-free mode and perform bounce oscillations between their mirror points (Fig. 1, *b*). Their initial angular spread is governed by geometric focusing of the heating injector beams and amounts to several degrees. Kinetics of the energy relaxation of ions is determined by their cooling on warm plasma electrons and scattering on ions. Characteristic time of the fast deuterium ion stopping on electrons 100 eV in energy and $2\cdot 10^{13}$ cm^{-3} in concentration is estimated as ~ 6.3 ms, while characteristic time of fast ion scattering on target plasma ions is two orders of magnitude longer. Thus, the ratio of the fast ion energy and electron concentration and temperature is such that fast ions retain a small angular spread during the entire plasma discharge.

One of the main items of the GDT research program is studying the effects associated with the fast anisotropic plasma component [1]. In the modes with maximal plasma parameters, GDT exhibits various-type microinstabilities caused by anisotropy of the fast-particle distribution function. Such instabilities induce fast particles angular scattering, scattering into the loss cone, and other effects. This work is devoted to the first experimental observation of the fast-particle distribution function modification caused by the Alfven ion-cyclotron instability.

Previously, the Alfven ion-cyclotron instability was studied at GDTs theoretically and experimentally [6,7]. Using an azimuthal set of high-frequency magnetic probes, the oscillations' mode composition and frequency (~ 1 MHz) were determined. The spectrum of ions scattered into the loss cone was measured. In previous experiments, no instability influence on such integral plasma parameters as the fast-particle energy content and fusion reaction yield was detected.

In this study, the recently created diagnostics of deuterium fusion reaction products was used in addition to the azimuthal assembly of magnetic probes [2]. The following reactions occur in plasma:

$$\mathrm{D}+\mathrm{D}\rightarrow {}^{3}\mathrm{He}\,(0.82\,\mathrm{MeV})+n\,(2.45\,\mathrm{MeV})\approx 50\,\%,$$

$$\mathrm{D}+\mathrm{D}\rightarrow \mathrm{T}\,(1.01\,\mathrm{MeV})+p\,(3.02\,\mathrm{MeV})\approx 50\,\%.$$

Since both reaction cross-sections are almost equal in the energy range up to 100 keV, it is possible to detect one of the products and make conclusions about the total

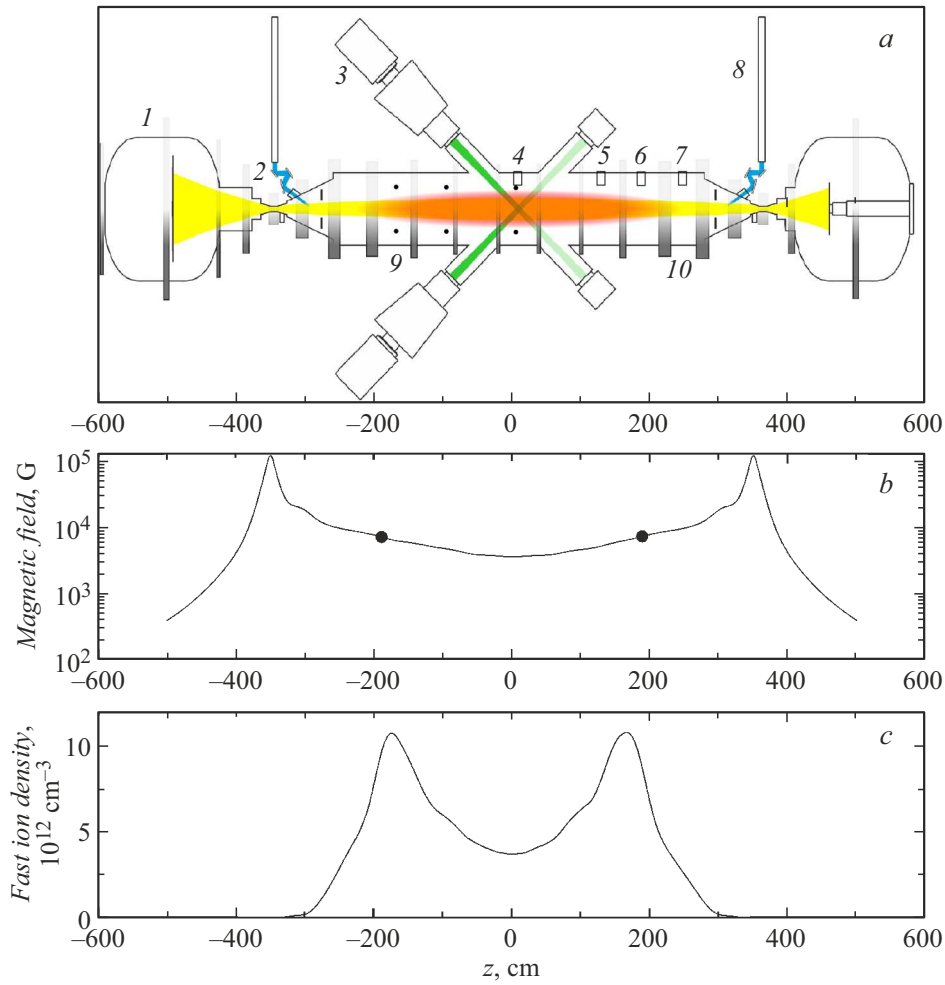

Figure 1. *a* — the GDT setup layout. *1* — vacuum tank of the plasma receiver, *2* — plug assembly, *3* — heating atomic injector, *4* — proton detector in the center ($z = 0$), *5* — proton detector at $z = 125$ cm, *6* — proton detector near the fast-particle mirror point $z = 175$ cm, *7* — proton detector at $z = 236$ cm, *8* — ECR heating line (ECR means the electron cyclotron resonance), *9* — diamagnetic loops at coordinate points $z = 0$, -100 and -180 cm, *10* — GDT central cell. *b* — GDT magnetic field. Dots indicate the field that is 2 times higher than that in the center (mirror points of fast deuterium ions). *c* — fast ion density calculated via code DOL.

number of reactions in the system. The diagnostics system for the GDT fusion reaction consists of several detector modules arranged along the setup at a variable pitch. The arrangement of detectors is shown in Fig. 1, *a*; they are designated by digits *4*–*7*. The detectors record 3.02 MeV protons. As the detectors, diodes with a thin dead layer of a large area (up to 1 cm^2) are used. The detector's entrance window is covered by aluminum foil 10 μm thick. The foil is not transparent to optical radiation, tritium, ^{3}He and atoms leaving the plasma; therefore, fusion reaction products other than the 3.02 MeV-protons were not detected in this study. Detection is performed in the mode of single particle counting , which allows measuring the absolute value of the DD reaction product flux without additional calibrations. Spatial resolution of up to several tens of centimeters is ensured by stainless-steel plate collimators installed in these experiments across the magnetic field.

Fig. 2, *a* presents a case oscillogram of a signal detected in the GDT experiment. Duration of the peak corresponding to a single proton is 50 ns. In addition, Fig. 2, *b* demonstrates a pulse spectrum obtained in detecting the 3.02 MeV protons. The amplitude distribution maximum is shifted by 0.23 MeV, which complies with the proton energy loss in the aluminum foil (10 μm). As per estimates, broadening of the 3.02 MeV line in the plasma with fast ions having initial energy of 22 keV and distribution function $f(v) \propto A/v^3$ is ~ 260 keV at half-maximum, which is consistent with the measured pulse amplitude spectrum ~ 300 keV. The only one amplitude-spectrum peak near 2.8 MeV evidences that other particles do not contribute to the measurements.

Fig. 3, *a* presents the time dependence of the fusion reaction yield measured by the fusion proton detectors. The diagnostics' time resolution is 0.1 ms; it is determined by the statistics collection time. At the moment of 6.2 ms, a sharp decrease in the number of events at the detector installed near the fast-particle mirror pointand synchronous increase in the count rate of detectors located in the GDT center and behind the fast-particle mirror point are observed.

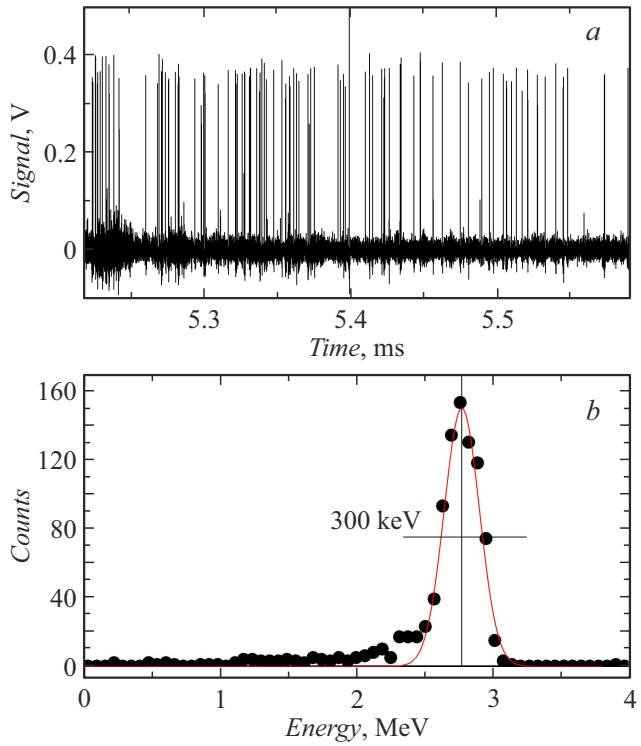

Figure 2. *a* — an example of a proton detector signal. *b* — amplitude spectrum obtained by detecting 3.02 MeV protons in the GDT discharge.

The diamagnetic loop near the mirror point (the loops arrangement is shown in Fig. 1, *a*) exhibits a signal decrease, while diamagnetic loops near the center exhibit a signal increase. This data is presented in Fig. 3, *b*. Analysis of the magnetic probe signals has shown an evolution of the Alfven ion-cyclotron instability. Note that, in experiments not demonstrating the instability evolution, each 3.02 MeV proton detector exhibits a proton yield monotonic growth throughout the entire operating period of heating injectors. An example of such an experiment is given in [2].

Fig. 4 presents the longitudinal profile of the fusion reaction yield before and after the instability development; the figure demonstrates a significant instability-induced decrease in the neutron yield peaking (the ratio between the signal on the detector near the mirror point and that from the central detector), which argues for a modification of the fast-particle distribution function.

To analyze the presented experimental data, the distribution function of fast particles was simulated via program code DOL [5]. In calculating the fast-ion distribution function, the setup geometric dimensions and magnetic field were used as the model input parameters (Fig. 1, *b*). The preset parameters were the injection energy and injector currents, as well as their angular spread. Among the results of calculation there is, e. g., time dependence of the electron temperature, which was consistent with measurements obtained in the GDT experiment. The fast-ion distribution function calculated using the DOL code for the initial heating injector angular spread of 3° is shown in Fig. 4, *b*. The data are presented for the time moment corresponding to the end of injection. The maximum concentration is observed in the phase space region near the point where injected atoms get captured (22 keV, 45°). In the process of cooling, fast ions are slightly scattered by angles; however, the distribution function remains far from Maxwellian. The absence of low-energy calculations in Fig. 4, *b* is explained by such a feature of code DOL as separate consideration of properties of the fast plasma component and parameters of the target plasma whose distribution function is Maxwellian. Note that this DOL code feature does not introduce a significant error into the below-presented calculated profiles of the fusion reaction yield, since the main contribution to the reaction is made by ions with energies close to that of injection, while the influence of target plasma properties is low. Then, the longitudinal profile of fusion reaction yield was calculated based on the obtained distribution function (reactions both between fast deuterium ions and between fast ions and target plasma ions were calculated). The model profile was normalized to the DD reaction yield measurements. Prior to the development of instability, the measurements and calculations were in good agreement (squares in Fig. 4, *a*).

Modern concepts of the Alfven ion-cyclotron instability allow concluding that the instability gives rise to angular scattering of fast particles with energies close to the injection energy [6,7]. To simulate the effect of instability on the distribution function, the initial angular spread of heating injector beams (one of the DOL code input parameters) was increased from 3° to 6° and 9°. Fig. 4, *a* presents longitudinal profiles of the fusion reaction yield for the given modeling conditions. The study has shown that broadening

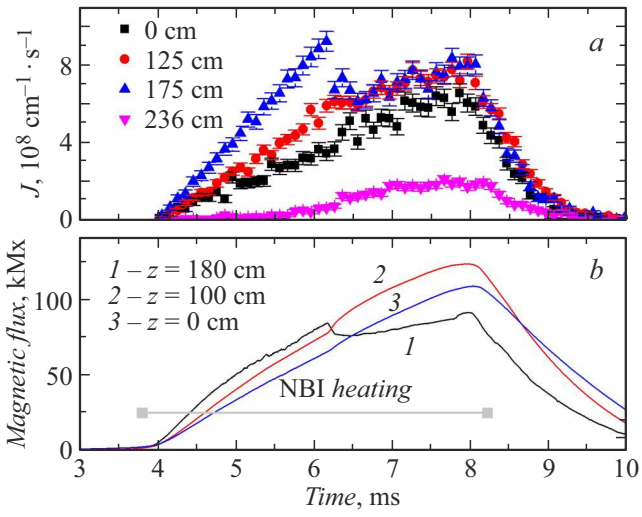

Figure 3. *a* — fusion reaction yield (per unit setup length) measured by the 3.02 MeV proton detectors located at different coordinates along the setup. *b* — magnetic flux displaced by the plasma (measured by the diamagnetic loops located at different coordinates along the setup). In addition, operating time of the plasma heating system is shown.

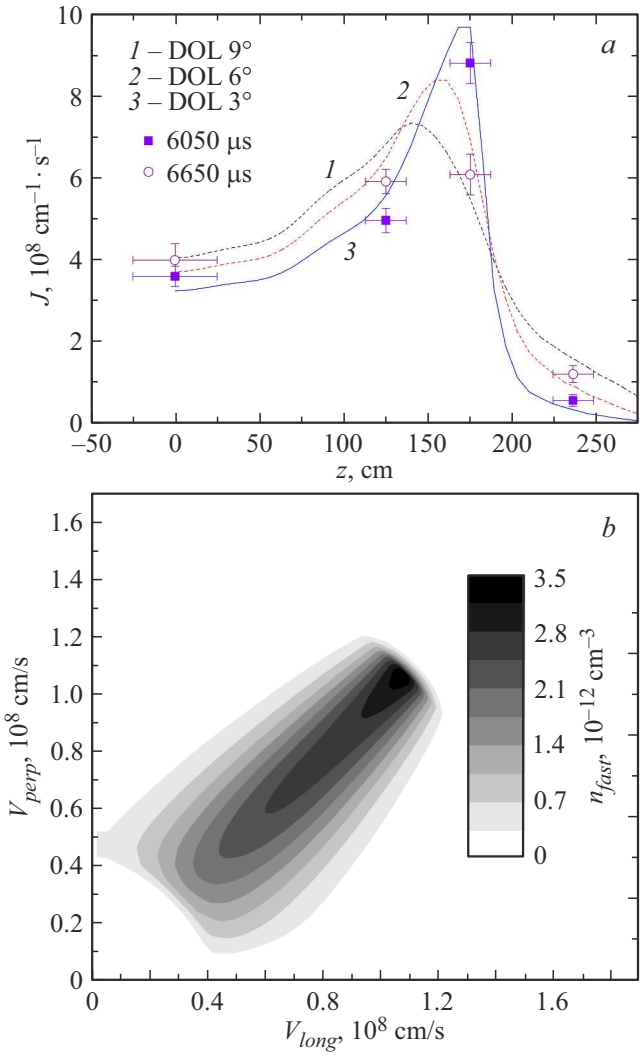

Figure 4. *a* — longitudinal profile of the fusion reaction yield before (squares) and after (circles) development of the Alfven ion-cyclotron instability. The curves represent the results of simulation via code DOL [5] for the heating injectors' angular spread of 3 to 9°. *b* — fast-ion distribution function in GDT(calculated via code DOL).

of the fast-particle angular distribution function leads to a decrease in peaking, which was measured experimentally. Circles in Fig. 4, *a* represent the measured fusion reaction profile after the development of instability.

Thus, the diagnostics system for the fusion reaction in GDT made it possible to measure absolute values of the fusion reaction yield with spatial resolution of several tens of centimeters and to reveal modification of the longitudinal profile of the fusion reaction intensity. This modification was modeled by using the DOL code and appeared to be consistent with the angular broadening of the fast particle distribution function, which confirms the theory of Alfven ion-cyclotron instability. Application of the diagnostics to studying the influence of various microinstabilities on fast particles in GDT looks promising.

Conflict of interests

The author declares that he has no conflict of interests.

References

[1] A.A. Ivanov, V.V. Prikhodko, Phys. Usp., **60** (5), 509 (2017). DOI: 10.3367/UFNe.2016.09.037967.

[2] E.I. Pinzhenin, V.V. Maximov, Instrum. Exp. Tech., **67** (2), 240 (2024). DOI: 10.1134/S0020441224700490.

[3] E.I. Soldatkina, P.A. Bagryansky, E.D. Gospodchikov, P.V. Zubarev, S.V. Ivanenko, A.N. Kvashnin, O.A. Korobeynikova, L.V. Lubyako, V.V. Maximov, D.V. Moiseev, S.V. Murakhtin, A.K. Meyster, E.I. Pinzhenin, V.V. Prikhodko, E.A. Puryga, A.L. Solomakhin, A.D. Khilchenko, V.A. Khilchenko, T.A. Khusainov, A.G. Shalashov, E.A. Symigelsky, Plasma Phys. Rep., **51** (9), 999 (2025). DOI: 10.1134/S1063780X25603852

[4] P.A. Bagryansky, A.V. Anikeev, G.G. Denisov, E.D. Gospodchikov, A.A. Ivanov, A.A. Lizunov, Yu.V. Kovalenko, V.I. Malygin, V.V. Maximov, O.A. Korobeinikova, S.V. Murakhtin, E.I. Pinzhenin, V.V. Prikhodko, V.Ya. Savkin, A.G. Shalashov, O.B. Smolyakova, E.I. Soldatkina, A.L. Solomakhin, D.V. Yakovlev, K.V. Zaytsev, Nucl. Fusion, **55**, 053009 (2015). DOI: 10.1088/0029-5515/55/5/053009

[5] D.V. Yurov, V.V. Prikhodko, Yu.A. Tsidulko, Plasma Phys. Rep., **42** (3), 210 (2016). DOI: 10.1134/S1063780X16030090.

[6] Yu.A. Tsidulko, I.S. Chernoshtanov, Plasma Phys. Rep., **40** (12), 955 (2014). DOI: 10.1134/S1063780X1412006X.

[7] K.V. Zaytsev, A.V. Anikeev, P.A. Bagryansky, A.S. Donin, O.A. Korobeinikova, M.S. Korzhavina, Yu.V. Kovalenko, A.A. Lizunov, V.V. Maximov, E.I. Pinzhenin, V.V. Prikhodko, E.I. Soldatkina, A.L. Solomakhin, V.Ya. Savkin, D.V. Yakovlev, Phys. Scripta, **2014** (T161), 014004 (2014). DOI: 10.1088/0031-8949/2014/T161/014004

Translated by EgoTranslating